Eur. Phys. J. E **3**, 87–97 (2000)

THE EUROPEAN PHYSICAL JOURNAL E

EDP Sciences

Droplet suction on porous media

L. Bacri and F. Brochard-Wyart[a]

Laboratoire Physico-Chimie Curie - Unité Mixte de Recherche 168, Centre National de la Recherche Scientifique/Institut Curie, 26 rue d'Ulm, 75248 Paris Cedex 05, France[b]

Received 19 January 2000

Abstract. We study the forced aspiration of small (≈ mm) and large (≈ cm) liquid drops, deposited on prewetted porous membranes, and pumped mechanically with a constant current J. Two kinds of membranes are used where the pores are i) disconnected, cylindrical and calibrated or ii) interconnected "sponge-like". Whatever the size of the drops and the intensity J of the current, two suction regimes are observed *versus* time: 1) a "*locked*" regime, when the drop is pinned, with a dynamic contact angle decreasing from advancing (θ_a) to finite receding (θ_r) contact angle; 2) an "*unlocked*" regime, where the contour line recedes with a constant contact angle closed to θ_r. In both regimes, the shape of the drop remains quasistatic, during the suction process, *i.e.* a spherical cap for small drops and a flat "gravity pancake" for large ones.

PACS. 68.45.Gd Wetting – 47.55.Mh Flows through porous media

1 Introduction

Wetting of porous media occurs in many industrial processes: oil recovery, textile technology, reprography and printing, dissolution of powders, protection of stone walls in building, etc.

In some cases such as the 4-color offset printing, the porous material is covered by a water film. The water must be removed very fast when the sheets reach the desired printing roller. As described theoretically in [1], this is achieved by a dewetting of the intercalated film, assisted by a suction of the water in the hydrophilic paper.

Our aim here is to study the wetting and the dewetting of prewetted porous membranes. The removal of liquid films by dewetting on simple substrates (smooth, chemically homogeneous) is now well understood [2]. The case of real substrates (rough or dirty) has also been studied [3]: it is more complex because one must include the hysteresis of the contact angle. On the other hand, the removal of liquid film from a porous substrate has not yet been studied. We are faced with several difficulties: i) the surface is irregular and hysteresis effects cannot be avoided; ii) the wettability depends upon the degree of humidity: the contact angles θ_a and θ_r are different on dry and wet membranes.

The difficulties also show up in capillary penetration of liquid droplets deposited on *dry* porous media [4–6]. Marmur has incorporated hysteresis and finite-size effects on the penetration of a liquid droplet into a capillary tube [5] and into a so-called radial capillary [6]. The radial capillary consists of two parallel plates separated by a small distance, with one of the plates containing one single small hole. The liquid of a droplet situated above the hole is drawn into the space between the plates. This work has been extended to the case of a droplet deposited on a porous substrate with a collection of non-connected cylindrical pores distributed uniformly over the surface [4]. This represents a more realistic system, because the number of pores in contact with the drop decreases when the liquid is depleted. Two limit cases have been considered: i) Strong hysteresis, assuming that the receding contact angle is zero. The drop is pinned and depleted at constant area. ii) Weak hysteresis, when the drop is depleted at constant contact angle. Finally, the effect of pore connectivity has also been discussed, and the increase of rate of depletion predicted.

These works modelize the *spontaneous penetration* of a drop into a porous medium. The present article considers the *forced penetration* of a liquid droplet into a porous body. We suck in the liquid through it. One motivation was to test a recent theoretical model [7] for the forced suction of a droplet in the limit of strong hysteresis (zero contact angle): the radius associated with the effective area of the droplet is constant. The theoretical effort is essentially focused on the drop at early times: then, the prediction is that the drop does not remain spherical, a deformation should propagate from the outer rim towards the drop axis. But these early processes are very difficult to see. In this article, we observe the long time behavior. We do study the removal of liquid (spherical droplets or puddles) deposited on a porous membrane by

[a] e-mail: brochard@curie.fr

[b] In collaboration with Université Pierre et Marie Curie, 4 Place Jussieu, 75005 Paris, France.

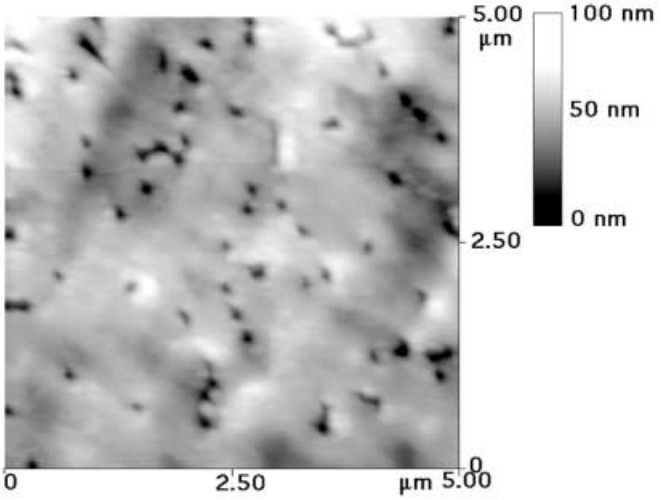

Fig. 1. AFM picture of well-separated pores in an isopore membrane (tapping mode).

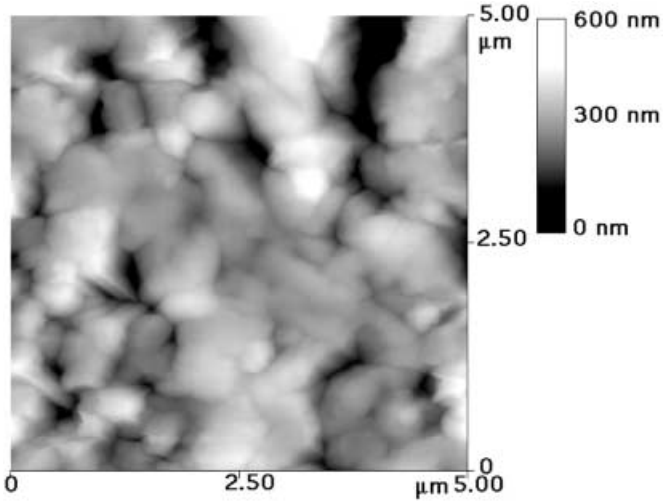

Fig. 2. AFM picture of interconnected pores in a durapore membrane (tapping mode).

pumping with a prescribed pressure drop ΔP. The hysteresis is large, but the receding contact angle is finite: this will lead to two suction regimes. We shall also use two types of membranes: with cylindrical pores or with interconnected pores in order to know the influence of the internal structure of the substrate. We vary also the viscosity of the liquid and the suction velocity.

2 Characterization of the porous membranes

2.1 Visualization of the pores

We use two types of membranes purchased by Millipore.

– The first one is called *isopore*: it is composed of non-connected vertical capillary tubes (cf. Fig. 1). It is made of polycarbonate and is hydrophilic. The vertical capillary tubes hinder the lateral diffusion: the suction will be always vertical. The pores diameter, deduced from our AFM picture is about 0.2 μm and the membrane thickness is 10 μm.
– The second one is called *durapore*. It is made of polyvinylidene fluoride (PVDF). The internal pore structure is sponge-like (cf. Fig. 2): the pores are interconnected. The pore size is about 0.22 μm and the membrane thickness is 140 μm. The membrane is hydrophobic.

2.2 Porosity, pore size and permeability

The porous media are characterized by their porosity ϕ, the pore size, the permeability $\mathcal{K}$.

The porosity is the ratio

$$\phi = \frac{\text{Pores volume}}{\text{Total volume}}\,.$$

In the case of the isopore membrane, the pores are non-connected vertical tubes, then we can write $\phi = \frac{\text{Pores surface}}{\text{Total surface}}$. We can easily measure from our AFM image the fraction of the occupied surface, which leads to the porosity ϕ and we find $\phi \sim 4\%$. In the case of the durapore membrane, the porosity is calculated by measuring the weigth of a wet and a dry membrane, it is about 75%.

The permeability $\mathcal{K}$ is given by Darcy's law [8] equation (1):

$$Q = \frac{\mathcal{K}}{\eta}\, S\, \frac{\Delta P}{L}\,, \tag{1}$$

where Q is the flow rate through the porous medium, S the area, L the thickness of the medium, η the viscosity of the liquid, ΔP the pressure drop (cf. Fig. 3).

Experimentally, the porous membrane is put on a disc of Teflon, in which we have made several holes (diameter 0.5 mm): we can apply high pressures (1 bar) without breaking the membrane. We put the system in a watertight cavity, in which we have pierced 4 holes (cf. Fig. 4). Two of them are used to obtain a flow rate Q through the membrane with a pump. We use a flowmeter to measure it. The two other holes are used to measure the difference of pressure ΔP trough the membrane with a pressure sensor.

For the measurements, we use water. We plot the flow rate Q as a function of the velocity $\frac{\Delta P\, S}{\eta\, L}$ (cf. Fig. 5). The curve is linear: the slope value is the membrane permeability given by Darcy's law (cf. Eq. (1)).

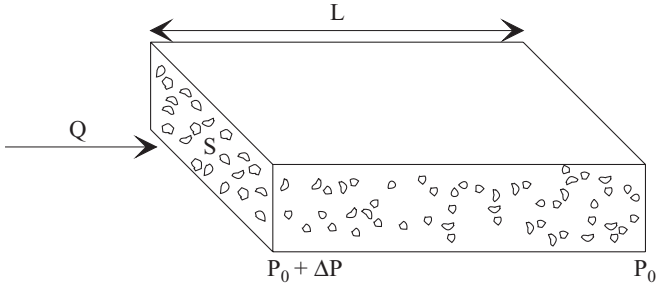

Fig. 3. Darcy's law.

Table 1. Physical properties of two water/glycerol mixtures.

% Glycerol	η (mPa s)	ρ (kg/m^3)	ν (cSt)	γ (mN/m)	κ^{-1} (mm)	$\frac{\gamma}{\eta}$ (m/s)
0%	1	1000	1	72.8	2.72	72.8
80%	55.48	1197.72	46.32	60.2	2.26	1.1

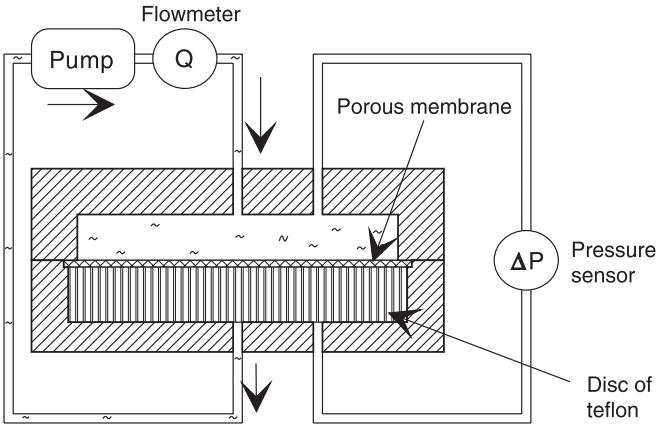

Fig. 4. Experimental setup to measure the permeabilities.

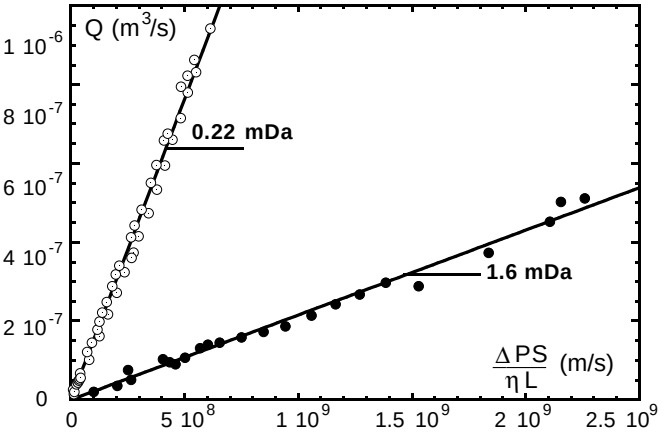

Fig. 5. Flow rate of water through an isopore • and a durapore ⊙ membrane *vs.* the velocity $\frac{\Delta P S}{\eta L}$.

We find a permeability to water: $\mathcal{K} = 0.22$ mDa (1 Da = 1 μm^2) for our isopore membrane (cf. Sect. 2.1). For the durapore membrane (cf. Sect. 2.1), the permeability to water is $\mathcal{K} = 1.6$ mDa.

2.3 Nature of the liquids

The liquids used are mixtures of water and glycerol. We choose two concentrations of glycerol (0% and 80%) in order to vary the viscosity of the liquid between 1 and 55.5 mPa s. The physical properties of these mixtures are written in Table 1.

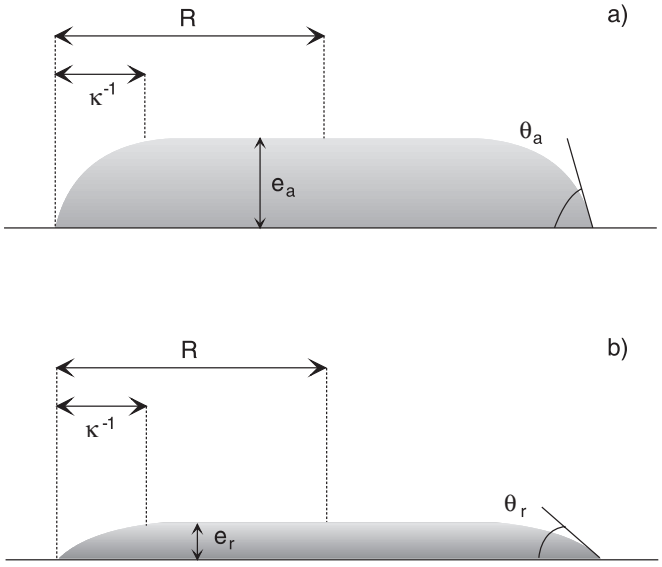

Fig. 6. Profile of a puddle in the advancing case a) and in the receding case b).

2.4 The advancing and receding angles

On real surfaces the equilibrium contact angle can take any value between an advancing angle θ_a and a receding angle θ_r: $\theta_r < \theta < \theta_a$. This angle depends on how the droplet was brought on the surface. We measure the advancing angle when the radius of the droplet increases if we increase its volume by adding liquid. The receding contact angle is measured when the radius of the droplet decreases by sucking liquid. The hysteresis is the difference between θ_a and θ_r. Why do we have hysteresis?

Real surfaces are irregular and dirty. Then, the liquid is pinned on defects. Most studies on hysteresis are based on two sorts of heterogeneous surfaces: rough or chemically heterogeneous. Our problem is different: the pores represent an extreme form of heterogeneity.

We determine θ_a and θ_r by measuring the thicknesses e_a and e_r of large drops flattened by gravity, called gravity pancake or puddles. Small drops achieve spherical cap and large drops are flattened.

The crossover radius between these capillary and gravity regimes is the capillary length $\kappa^{-1} = \sqrt{\frac{\gamma}{\rho g}}$ (where γ and ρ are the surface tension and the density of the liquid and g is the gravitational acceleration). The "gravity pancake" has at equilibrium a thickness e_0 which results from a balance between gravity and capillarity. The free

Table 2. Measurements of receding and advancing angles for pure water and mixture of water/glycerol (1:4) for both membranes and calculus of the critical thickness.

Water	θ_a (°) $\pm 1.4°$	θ_r (°) $\pm 1.9°$	e_a (mm) $\pm 55\,\mu$m	e_r (mm) $\pm 86\,\mu$m
Dry isopore	43.7		2	
Prewetted isopore	43.1	10.7	2	0.51
Dry durapore	90.2	21.2	3.9	1.00
Prewetted durapore	27.7	11.5	1.3	0.55
Water/Glycerol (1:4)				
Dry isopore	59.8		2.3	
Prewetted isopore	58.2	11	2.2	0.44
Dry durapore	92.9	13.9	3.3	0.54
Prewetted durapore	36.4	12.1	1.4	0.48

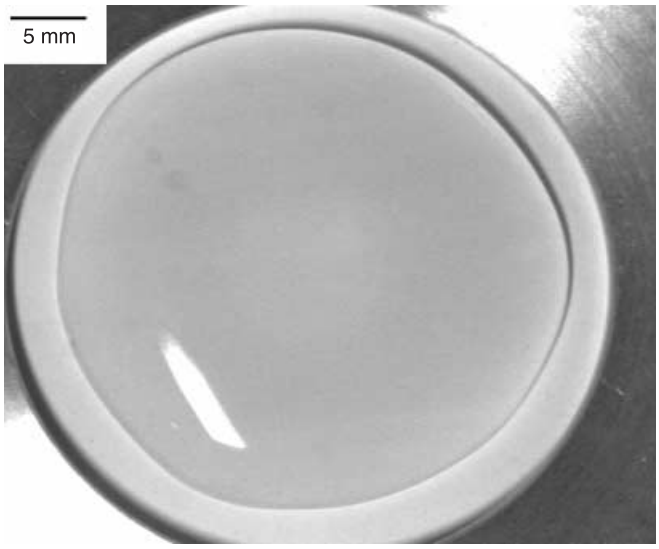

Fig. 7. Puddle of water on a dry isopore membrane.

energy $\mathcal{F}$ of the drop *vs.* thickness e can be written as

$$\mathcal{F} = \frac{1}{2}\rho g e^2 \frac{\Omega}{e} + \frac{\Omega}{e}(\gamma + \gamma_{SL} - \gamma_{SG}), \qquad (2)$$

where Ω is the liquid volume, e the thickness of the pancake, Ω/e the wet area and γ_{SG}, γ_{SL} and γ the solid/gas, solid/liquid and liquid/gas interfacial tensions. Minimizing (2) with respect to e gives a formula for e_0:

$$e_0 = \sqrt{2\frac{-\mathcal{S}}{\rho g}}, \qquad (3)$$

where $\mathcal{S}$ is the spreading coefficient, defined by $\mathcal{S} = \gamma_{SG} - (\gamma_{SL} + \gamma)$. We can also write the spreading coefficient $\mathcal{S}$ as a function of the contact angle θ_0 of the droplet on the substrate (via Young's relation) and we deduce

$$e_0 = 2\,\kappa^{-1} \sin\left(\frac{\theta_0}{2}\right). \qquad (4)$$

In the case of our membranes, the hysteresis is high. Then, we have two limit thicknesses values: the first one, which depends on the advancing angle, is $e_a = 2\,\kappa^{-1} \sin\left(\frac{\theta_a}{2}\right)$ and the second one, which depends on the receding angle, is $e_r = 2\,\kappa^{-1} \sin\left(\frac{\theta_r}{2}\right)$ (cf. Tab. 2). The pancakes can have all thicknesses between the two limits e_r and e_a (cf. Fig. 6).

For the advancing case, we film the surface S from above with a camera and we measure its weight (*i.e.* the volume Ω) with a balance. From these measurements, we can calculate the thickness $e_a \cong \frac{\Omega}{S}$ and the contact angle θ_a of the puddle (cf. Eq. (4) and Fig. 7). For the receding case, the thickness of the puddle is too thin to obtain a good contrast by filming from above with the camera. That is why we measure the thickness e_r by filming from the side the profile of the puddle. We calculate the contact angle θ_r by using the formula equation (4). We do the measurements on the porous media with droplets of pure water and of a mixture of glycerol and water, composed by 80% of glycerol (cf. Tab. 2). We have studied both the dry and the prewetted membranes (the hysteresis of the prewetted membranes is lower). The advancing angle of the dry durapore membrane is about 90° and the receding angle is about 21°. Then, the hysteresis is high (69°). On the dry hydrophilic isopore membranes, the advancing contact angle is $\theta_a^{Dry} = 43.7°$, but the receding contact angle θ_r^{Dry} cannot be measured because the membrane is hydrophilic.

2.5 Stability of liquid films

The equilibrium thickness e_r is also the critical thickness for dewetting [9]. A film deposited on a solid substrate is metastable below this critical thickness e_r. If the thickness e of the film is smaller than e_r, we observe a dewetting of the film by nucleation and growth of a dry patch, as shown in Figure 8. Spontaneous and "forced" dewetting on porous membranes will be described in a separate paper.

3 Experiments on suction

3.1 Experimental setup

If we apply the pressure difference $\Delta P = \rho g h$ on a bare membrane, it bends. In order to avoid this, we put the

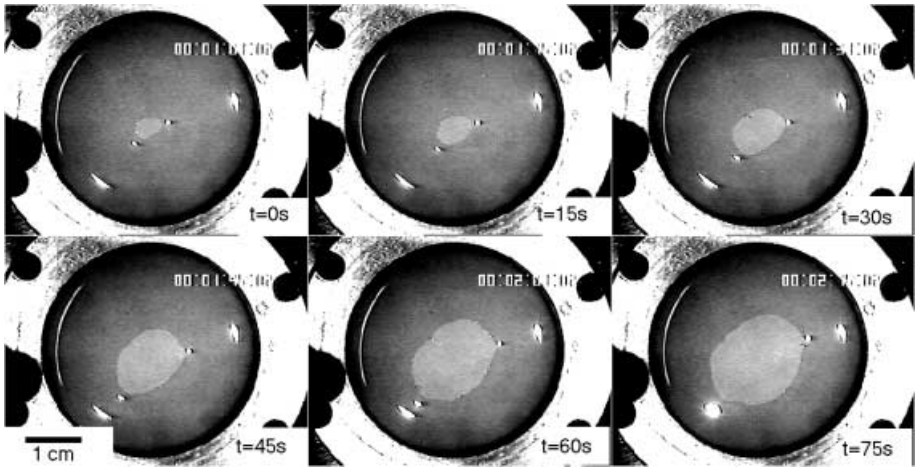

Fig. 8. Dewetting of a water film on a prewetted durapore membrane.

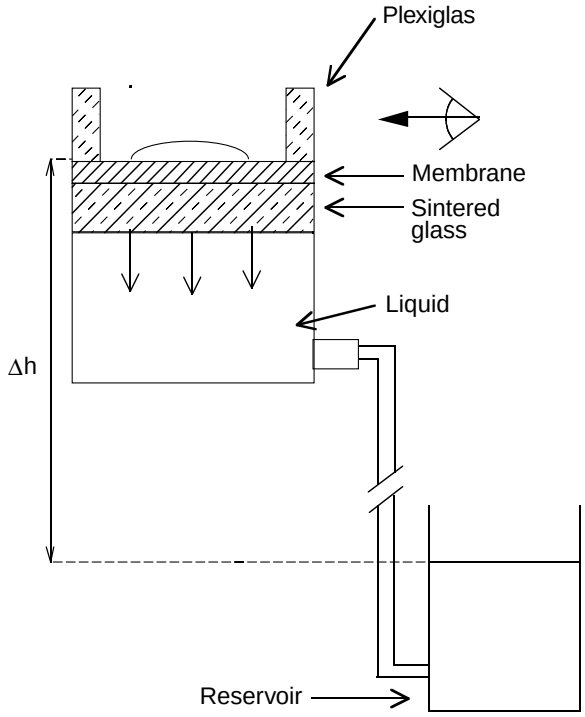

Fig. 9. Experimental setup for the wetting study.

membrane on a support made of sintered glass (pores diameter: 10–16 μm, cf. Fig. 9): now, the membrane is flat when we apply the pressure. We saturate the membranes in order to stick them (by capillarity). There are no air bubbles between the membrane and the sintered glass.

Experimentally, we saturate the membrane and the sintered glass with pure water from Millipore during 15 minutes. In the case of the hydrophobic membrane, we add a bit of absolute ethanol to the pure water. The porous membrane is maintained on a sintered glass plate. We deposit a droplet of liquid on the porous substrate, which is fixed by a clear Plexiglas rest with clean flat sides in order to film the droplet profile without distortion. The images acquired by the camera are analyzed afterwards by an image processing software (cf. Fig. 10). This gives a measure of the 3 variables: the radius R, the height h and the contact angle θ of the droplet with the substrate.

We naively thought that the droplet would have a bell-shape as predicted in reference [7]. But, the droplets are perfect spherical caps. It is therefore easy to calculate the volume Ω as a function of the radius R and the contact angle θ (cf. Fig. 11 and Eq. (5))

$$\Omega = \frac{\Pi\, R^3}{\sin^3\theta} \left\{ \frac{2}{3} + \left(\frac{1}{3}\cos^2\theta - 1 \right) \cos\theta \right\} . \qquad (5)$$

3.2 Volume measurements and Darcy's law

3.2.1 Isopore membrane

Using equation (5), we plot the time evolution of the volume of a droplet of a mixture of 80% of glycerol and of 20% of water (cf. Fig. 12) from the measurements of the radius R and the contact angle θ. The volume is decreasing linearly with time, and the slope of the line gives the suction flow rate Q. We begin again the experiments varying the pressure ΔP. The plot of the suction velocity $J = \frac{Q}{S}$ (where S is the contact area between the droplet and the porous substrate) as a function of $\frac{\Delta P}{\eta L}$ (cf. Fig. 13) is linear. We find Darcy's law again (cf. Eq. (1)) with a permeability $\mathcal{K} = 0.25 \pm 0.1$ mDa in good agreement with our direct measure (cf. Sect. 2.2). From this, we may deduce that the droplet suction follows very well the simple Darcy's law, because the contribution of the Laplace pressure ($\Delta P_{\rm L} \sim 2\,\frac{\gamma}{R}$) with $\gamma \sim 60 \cdot 10^{-3}$ Pa s and $R \sim 10^{-3}$ m is about 120 Pa, which is a negligible correction to the suction pressure $\Delta P \sim 5000$ Pa.

3.2.2 Durapore membrane

As for the previous experiment, we measure the volume of the droplet, which decreases linearly *versus* time. From

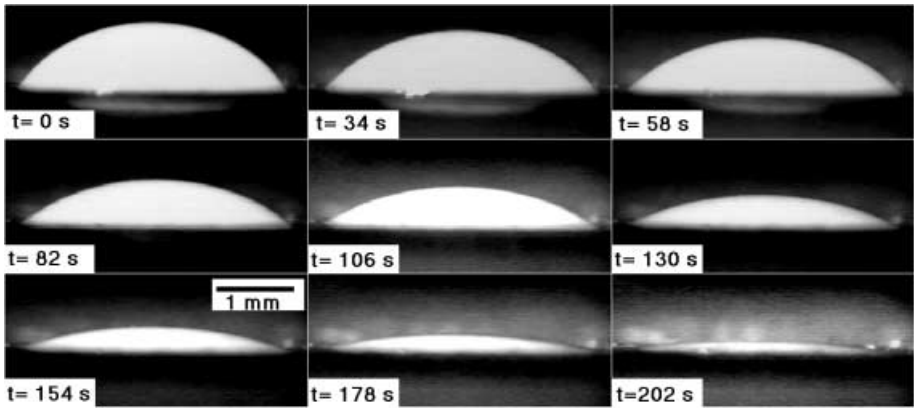

Fig. 10. Droplet of water-glycerol (80% glycerol) sucked by a pressure difference $\Delta P = 7490\,\mathrm{Pa}$ on an isopore membrane.

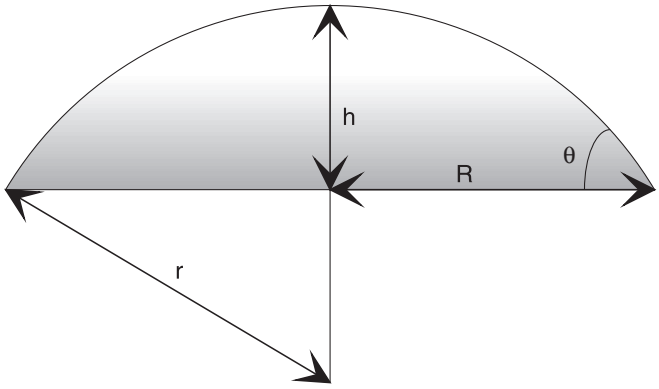

Fig. 11. A droplet as a spherical shape.

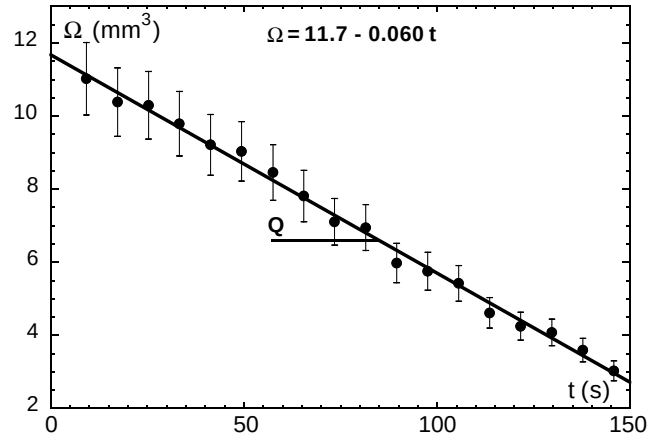

Fig. 12. Droplet volume of a mixture water/glycerol (80% of glycerol, 20% of water) sucked by a pressure difference $\Delta P = 7492\,\mathrm{Pa}$ on an isopore porous membrane.

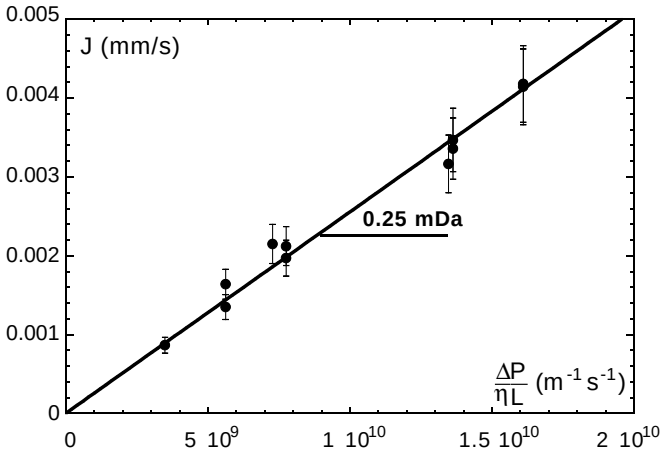

Fig. 13. Suction velocity as a function of $\frac{\Delta P}{\eta L}$ for an isopore membrane.

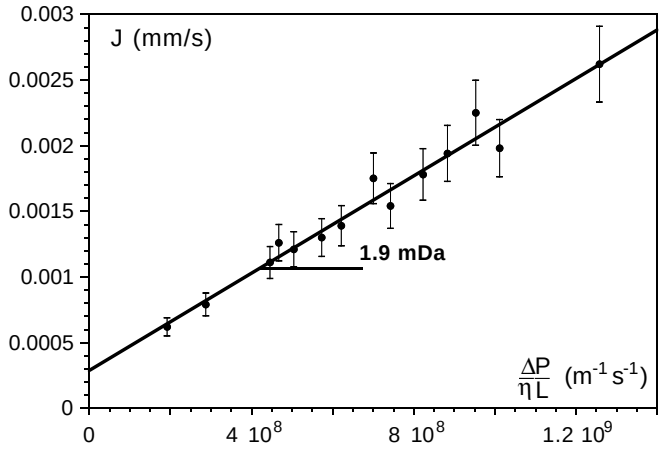

Fig. 14. Suction velocity as a function of $\frac{\Delta P}{\eta L}$ for a durapore membrane.

this, we deduce the suction velocity J and then the measured permeability, equal to 1.8 mDa for the pure water and 1.9 mDa for the mixture water-glycerol (1:4) (cf. Fig. 14). There is not an influence of the pore size of the sintered glass. We can remark that the measurements are in good agreement with our direct measure (cf. Sect. 2.2). The sintered glass does not influence the permeation through the membrane, what we have expected. The error is about 0.2 mDa. In the case of a hydrophobic membrane, the droplet suction follows well the simple Darcy's law.

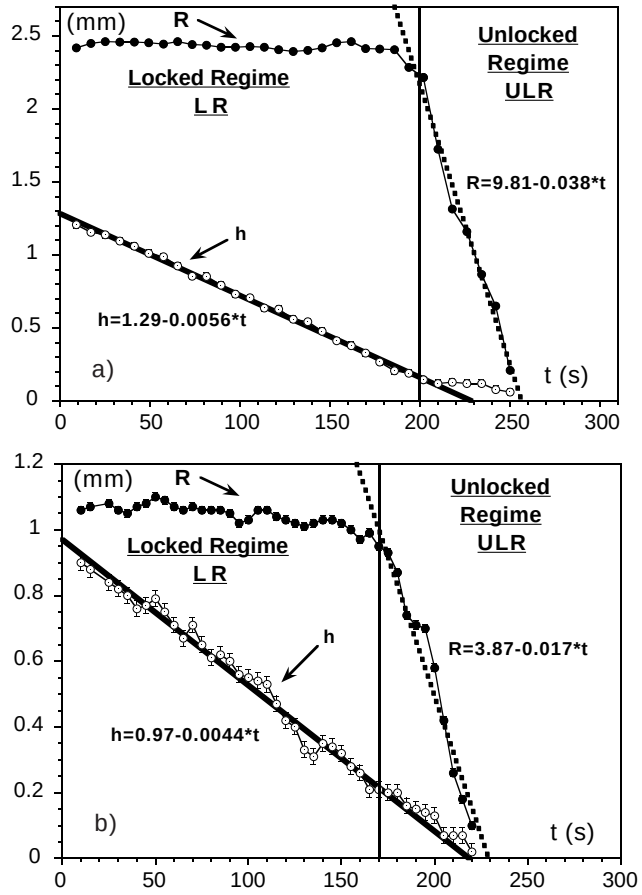

Fig. 15. Evolution of the radius R (•) and of the thickness h (⊙) of a droplet made up of 80% of glycerol and of 20% of water, put on an isopore membrane with a pressure $\Delta P = 7492\,\mathrm{Pa}$ (a) and on a durapore membrane $\Delta P = 4385\,\mathrm{Pa}$ (b).

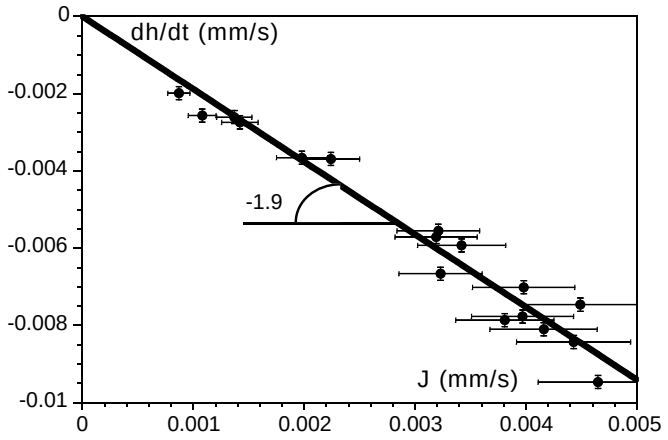

Fig. 16. Decrease velocity of the thickness h of the droplet as a function of the suction velocity.

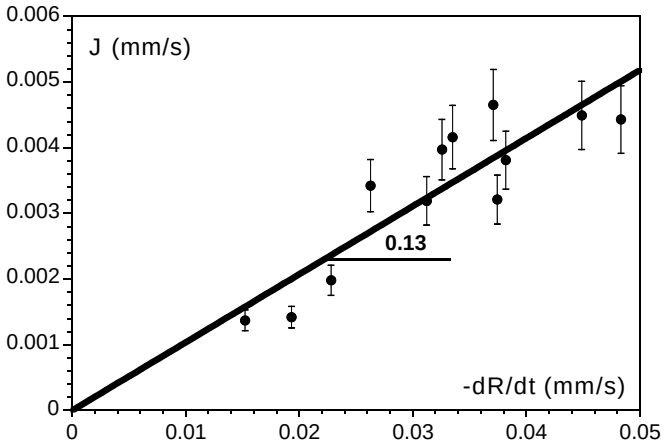

Fig. 17. Suction velocity as a function of the velocity of the decrease of the droplet radius (water/glycerol 1:4).

3.3 Suction of a small droplet

Now, we take an interest in the behavior of the radius R and of the thickness h of the sessile droplet with time (cf. Fig. 15) in the case of the capillary regime ($R \ll \kappa^{-1}$).

We find two regimes:

- $\theta > \theta_\mathrm{r}$, R is steady. The contact area S between the droplet and the porous substrate remains constant: the contact line is pinned by the surface defects. We call this regime the *Locked Regime* (LR).
- $\theta = \theta_\mathrm{r}$, R is decreasing. As the dynamical contact angle becomes small enough, Laplace force overcomes anchorage forces and the contact line moves. We call this regime the *UnLocked Regime* (ULR).

- The Locked Regime
  The radius R of the droplet is steady, but the thickness decreases linearly with time (cf. Fig. 15). We vary the suction flow rate Q and we plot $\frac{\mathrm{d}h}{\mathrm{d}t}$ as a function of the suction velocity $J = \frac{Q}{\Pi R^2}$ (cf. Fig. 16). We obtain a line with a slope of about -1.9. Then, $\frac{\mathrm{d}h}{\mathrm{d}t} \approx -1.9 \cdot J$, with both membranes and the sintered glass disc with the small pore size. With the durapore membrane and the sintered glass disc with large pore size, $\frac{\mathrm{d}h}{\mathrm{d}t} \approx -2.1 \cdot J$.

- The UnLocked Regime
  Now, the droplet radius decreases linearly with time (cf. Fig. 15). We plot the suction velocity J as a function of the velocity $\frac{\mathrm{d}R}{\mathrm{d}t}$ (cf. Fig. 17). The curve can be fitted by a line.

3.4 Suction of a puddle

In this paragraph, we study the behavior of the thickness e, the radius R and the contact angle θ of a flat puddle ($R \gg \kappa^{-1}$): it is the gravity regime.

We put a large amount of water (volume is about $1.5\,\mathrm{cm}^3$) on an isopore membrane. We measure the radius of the puddle *versus* time (cf. Fig. 18) and we vary the applied pressure (cf. Fig. 19).

- The Locked Gravity Regime
  At the beginning of the suction process, the radius of the pancake is constant. The thickness decreases linearly with time. The rate of decrease of the thickness $-\frac{\mathrm{d}e}{\mathrm{d}t}$ is a linear function of the applied pressure ΔP (cf. Fig. 20).

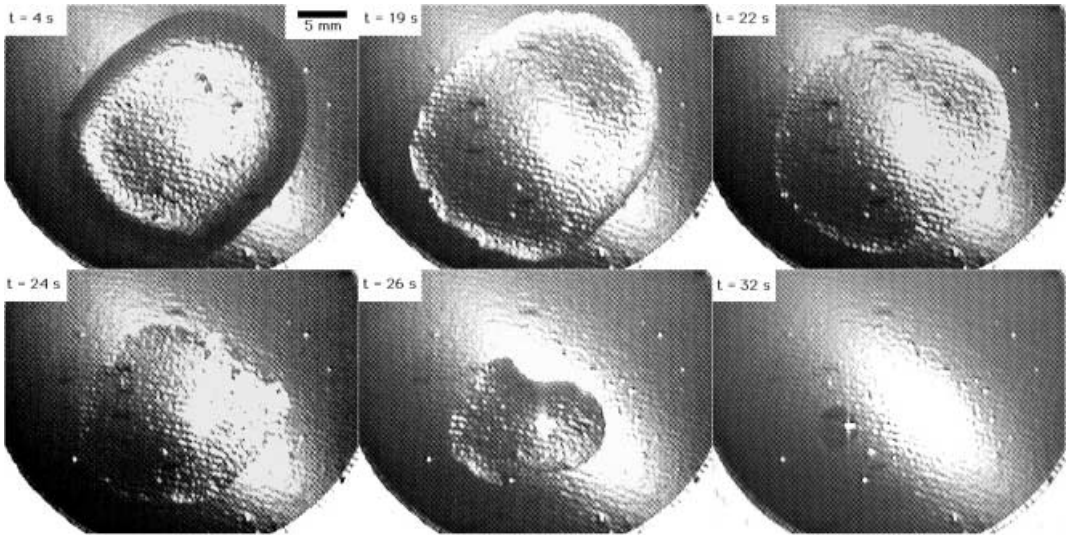

Fig. 18. Water pancake on an isopore membrane during time ($\Delta P = 2650\,\mathrm{Pa}$).

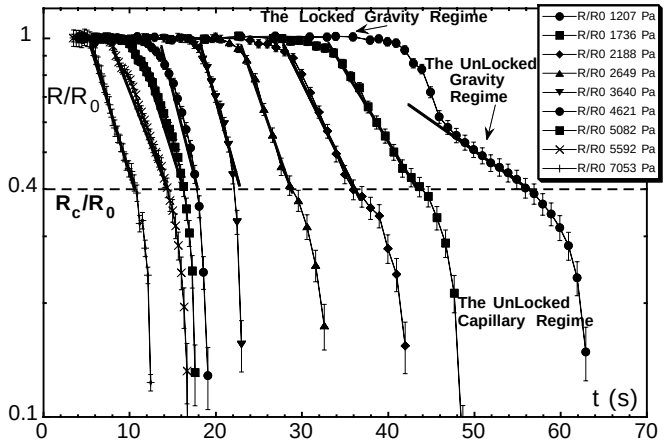

Fig. 19. Radius of the pancake during time when we increase the suction velocity.

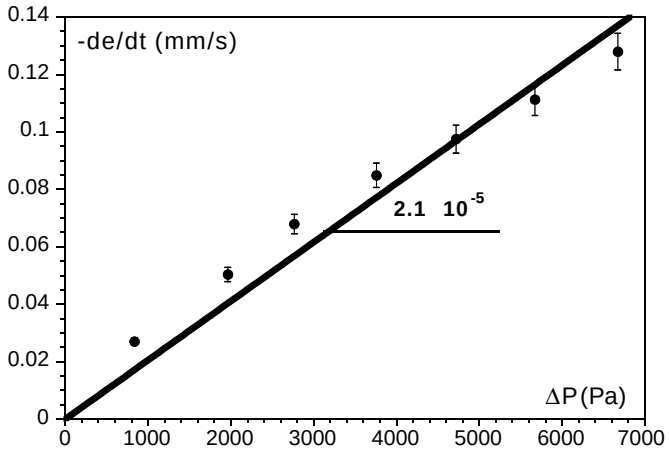

Fig. 20. Rate of thinning of a pancake as a function of the applied pressure.

- The UnLocked Gravity Regime
  At later times, the radius is not constant and decreases exponentially with time:

$$R = R_0 \exp\left\{-\frac{t - t_0}{\tau}\right\}.$$

  We plot τ as a function of the inverse of the applied pressure (cf. Fig. 21) and we find $\tau \approx \frac{4.1 \cdot 10^4}{\Delta P}$.

When the radius is smaller than $R_c \approx 4.8\,\mathrm{mm} = 2\,\kappa^{-1}$, the radius decreases linearly with time: we return to the capillary (unlocked) regime studied in Section 3.3.

4 Discussion

We study the behavior of a droplet placed on a porous membrane and sucked through it. The suction through the pores is opposing the spreading.

4.1 The Locked Regime

The droplet is spread, but its edges are attached to the surface because of the hysteresis of the contact angle: its radius R remains constant (cf. Fig. 22 (a)). The droplet is sucked through the porous medium with the velocity J. Its volume Ω decreases, then there is a variation of its height h and of the contact angle θ between the droplet and the porous membrane. The volume variation is given by

$$\frac{\mathrm{d}\Omega}{\mathrm{d}t} = -J \cdot \Pi R^2\,. \tag{6}$$

However, the droplet volume is given by (in the small angles approximation)

$$\Omega \cong \frac{\Pi}{4}\theta R^3\,. \tag{7}$$

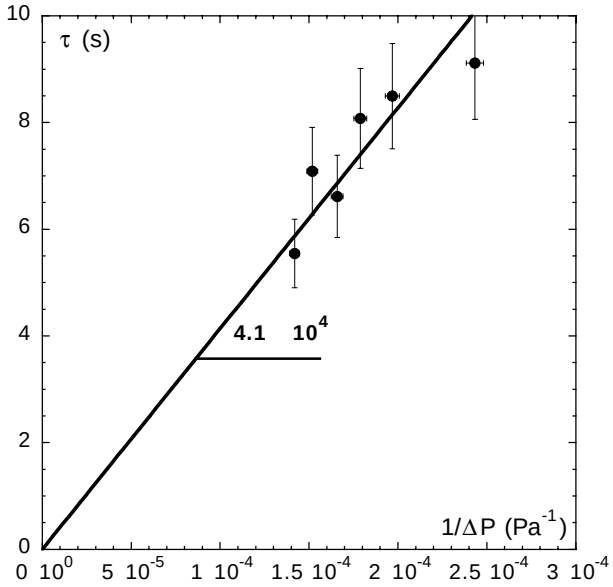

Fig. 21. τ as a function of the applied pressure ΔP.

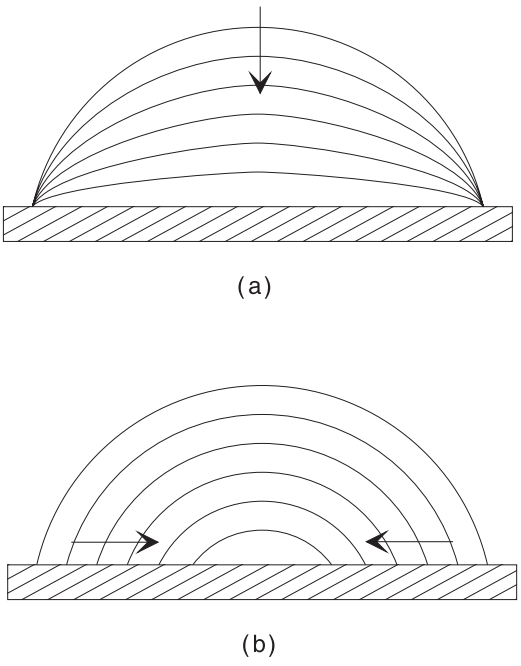

Fig. 22. (a) The Locked Regime, (b) the UnLocked Regime.

Substituting equation (7) into equation (6), one obtains the expression

$$\frac{R}{2}\frac{\mathrm{d}\theta}{\mathrm{d}t} \cong -2J\,.$$

But, there is a relation between the height h and the contact angle θ: $h = R\,\tan\left(\frac{\theta}{2}\right)$. Then, $\frac{\mathrm{d}h}{\mathrm{d}t} = \frac{R}{2\cdot\cos^2\theta}\,\frac{\mathrm{d}\theta}{\mathrm{d}t} \cong \frac{R}{2}\frac{\mathrm{d}\theta}{\mathrm{d}t}$, which leads to

$$\frac{\mathrm{d}h}{\mathrm{d}t} \cong -2\,J\,, \tag{8}$$

$$h \cong h_{(t=0)} \;-\; 2J\,t\,.$$

Experimentally, the radius R of the droplet remains constant and the thickness h decreases linearly with time (cf. Fig. 15). We have plotted $\mathrm{d}h/\mathrm{d}t$ as a function of the suction velocity J (cf. Fig. 16): it is a line with a slope equal to -2 ± 0.1. Equation (8) is correct within an error of 5%. We have checked that the contact angle θ decreases linearly with time.

4.2 The UnLocked Regime

Let us first remind the dynamics of contact lines. The advancing and receding motion of contact line on model surfaces such as silanized glass or silicon wafers is now well understood [10]. In the case of the partial wetting, a sessile droplet forms at equilibrium a spherical shape, characterized by an equilibrium contact angle θ_e. If the angle θ is different from θ_e, the contact line moves at a velocity $U(\theta)$. The motion equation relating the velocity U to the dynamic contact angle θ is obtained from the balance of two forces:

i) The *driving force* F: $F = \gamma(\cos\theta_\mathrm{e} - \cos\theta)$ is the non-compensated Young Force [2].
ii) The *friction force* F_v: at small θ we expect the losses to be dominated by viscosity: $F_\mathrm{v} = 3\eta\,\frac{U}{\theta}\,l_n$, where η is the viscosity of the droplet and l_n is a logarithm factor which depends on the solid/liquid system ($5 \leq l_n \leq 15$).

Equating the two forces F and F_v, we find the spreading velocity

$$U = \frac{V^*}{3\,l_n}\,(\cos\theta_\mathrm{e} - \cos\theta)\,\theta\,, \tag{9}$$

where $V^* = \frac{\gamma}{\eta}$ is a characteristic velocity. The motion of a contact line on a substrate with large hysteresis, such as a porous membrane, is more subtle, because one must take into account the pinning of the contact line to the surface defects [11]. When the line retracts (cf. Fig. 22 (b)), the equilibrium contact angle θ_e becomes the receding contact angle θ_r. One shall include the hysteresis by replacing θ_e by θ_r in the dynamical equation (9):

$$U = \frac{V^*}{3\,l_n}\,(\cos\theta - \cos\theta_\mathrm{r})\,\theta\,. \tag{10}$$

For our sucked droplets [12], $U \sim \frac{J}{\theta} \ll V^*$. According to equation (10), we shall assume that the dynamical contact angle is $\theta = \theta_\mathrm{r}$.

Now, we must take the equations of the volume variation equation (6) and equation (7) into account, in order to write the variation of the radius R, assuming a constant dynamical contact angle

$$\frac{\mathrm{d}R}{\mathrm{d}t} \cong -\frac{4}{3}\frac{J}{\theta_\mathrm{r}}\,, \tag{11}$$

then

$$R \cong R_{(t=0)} \;-\; \frac{4}{3}\,\frac{J}{\theta_\mathrm{r}}t\,.$$

Table 3. Angles deduced from the observed retractation of droplets.

Angles (°)	water ± 2	water/glycerol (1:4) ± 2	θ_r water ± 1.8	θ_r water/glycerol (1:4) ± 1.4
Isopore	13.2	10	10.7	11.0
Durapore	12.8	10.5	11.5	12.1

We plot the suction velocity J as a function of $\frac{dR}{dt}$ (cf. Fig. 17). The points are somewhat scattered. In fact, when the radius decreases, the droplet height is very small and it is difficult to measure exactly the parameters. The slope of this line is equal to $\frac{3}{4}\,\theta_r$ according to equation (11). Then, we find $\theta_r \approx 10°$. We make again the calculation for both porous membranes (isopore and durapore) and for both liquids (pure water and water/glycerol 1:4) (cf. Tab. 3).

The results are satisfactory in all cases.

4.3 Macroscopic pancakes

4.3.1 The Locked Gravity Regime

We put a pancake on the substrate and we pump it with the velocity J. At first, its edge is pinned. Its radius R_0 is constant and its volume is equal to $\Pi R_0^2\, e$, where e is the thickness. The rate of change of the volume Ω is

$$\frac{d\Omega}{dt} = \Pi R_0^2 \frac{de}{dt} = -J\,\Pi R_0^2\,.$$

Thus,

$$\frac{de}{dt} = -J\,, \qquad (12)$$
$$e = e_0 - J\,t\,.$$

Assuming a quasistatic equilibrium shape, we can write the relation between e and the contact angle θ: $e = \kappa^{-1}\,\theta$. Then, we can describe the decrease of the contact angle

$$\theta = \theta_a - J\kappa\,t\,. \qquad (13)$$

The angle θ decreases up to the value of the receding contact angle θ_r and the thickness e to the critical thickness $e_r = \kappa^{-1}\theta_r$.

Experimentally, we see that the velocity $\frac{de}{dt}$ decreases linearly with the pressure ΔP (cf. Fig. 20). But, (12) can be written taking account of (1) as a function of ΔP: $-\frac{de}{dt} = \frac{\mathcal{K}}{\eta\,L}\,\Delta P$.

Then, we can calculate $-\frac{de}{dt}$ (mm/s) $\approx 2.2 \cdot 10^{-5}\,\Delta P$. The slope of the line of Fig. 20 is about $2.1{\cdot}10^{-5}$, the result is in good agreement with our theoretical calculation.

4.3.2 The UnLocked Gravity Regime

When the contact angle is close to the receding angle, the radius R decreases. The thickness remains constant and equal to $e_r = \kappa^{-1}\,\theta_r$. The pancake volume is given by

$$\Omega = \Pi R^2\,e_r\,. \qquad (14)$$

Substituting equation (14) into equation (6), one obtains the expression

$$\frac{dR}{R} = \frac{-J}{2e_r}\,dt\,.$$

We integrate this equation with the condition $R = R_0$ when $t = t_0$:

$$R = R_0\,\exp\left\{-\frac{t-t_0}{\tau}\right\}, \quad \text{where} \quad \tau = \left|\frac{2e_r}{J}\right|. \qquad (15)$$

We have found that τ was proportional to the inverse of the applied pressure ΔP (cf. Fig. 21) and we know the permeability $\mathcal{K}$ of the membrane isopore, then we can calculate the thickness e_r of the pancake using (15) and (1): $e_r \approx \frac{4.1\cdot 10^4}{2}\,\frac{\mathcal{K}}{\eta L}$. We find $e_r \approx 0.45$ mm.

During this regime, we record on film the profile of the pancake and measure its thickness, which is about 0.5 ± 0.02 mm. This measure is in good agreement with our simple calculation.

When the radius is close to the capillary length, we return to the regime of the small drops where the capillary forces are dominant. Then, the radius of the droplet decreases linearly with time (cf. Eq. (11)).

5 Conclusion

In this work, we have studied the suction of two liquids: pure water and a mixture of water and glycerol with 80% of glycerol, in two porous media: the first with parallel pore structure (isopore) and the second with interconnected pores (durapore).

In the suction of small spherical droplets, we have seen two regimes: the *Locked Regime*: the droplet radius remains steady and its thickness decreases linearly with time, and the *UnLocked Regime*: the contact angle θ remains steady and the radius R decreases. Moreover, we have checked that while the droplet was shrinking, its contact angle was about equal to the receding angle.

In the suction of flat puddles, we observed three regimes: the *Gravitational Locked Regime*: the radius remains constant and the thickness decreases linearly with time; the *Gravitational UnLocked Regime*: the radius follows an exponential law as a function of time; and, when the radius is smaller than the capillary length κ^{-1}, the *UnLocked Regime* of the capillary regime. All our results can be interpreted assuming a quasiequilibrium shape for the drops and a Darcy law for the suction. Unfortunately, the transient regime studied in reference [7] is too short to be seen. If a suction velocity J is applied at time $t = 0$,

they predict that the signal propagates from the contact line at a velocity $V^* \theta_e^3$, which leads to a transient time $\tau \sim \frac{R}{V^* \theta_e^3} \sim 1\,\mathrm{ms}$.

References

1. P.G. de Gennes, C. R. Acad. Sci. Paris **318**, 1033 (1994).
2. F. Brochard-Wyart, P.G. de Gennes, Adv. Colloid Interface Sci. **39**, 1 (1992).
3. P.G. de Gennes, Rev. Mod. Phys. **57**, 827 (1985).
4. M. Denesuk, G.L. Smith, B.J.J. Zelinski, N.J. Kreidl, D.R. Uhlmann, J. Colloid Interface Sci. **158** 114 (1993).
5. A. Marmur, J. Colloid Interface Sci. **122**, 209 (1988).
6. A. Marmur, J. Colloid Interface Sci. **124**, 301 (1988).
7. A. Aradian, E. Raphaël, P.G. de Gennes, Eur. Phys. J. E **2**, 367 (2000).
8. E. Guyon, J.-P. Hulin, L. Petit, *Hydrodynamique physique* (InterEditions/Editions du CNRS, 1991).
9. C. Redon, F. Brochard-Wyart, F. Rondelez, Phys. Rev. Lett. **66**, 715 (1991).
10. L. Taner, J. Phys. D **12**, 1473 (1979).
11. E. Raphael, P.G. de Gennes, J. Chem. Phys. **90**, 7577 (1989).
12. If the moving liquid wedge is also sucked at velocity J, the motion of the contact line at velocity U includes both horizontal and vertical flow. Therefore the force balance (cf. Eq. (10)) has to be modified into $U - \frac{J}{\theta} = \frac{V^*}{3\,l_n}\,(\cos\theta - \cos\theta_r)\,\theta$.